Research Article

Integrative Cancer Therapies
2016, Vol. 15(4) 512–524

DOI: 10.1177/1534735416628273
ict.sagepub.com
SAGE

Evaluation of Antitumor Activity of Long-Circulating and pH-Sensitive Liposomes Containing Ursolic Acid in Animal Models of Breast Tumor and Gliosarcoma

Talita Guieiro Ribeiro Rocha, PhD[1], Sávia Caldeira de Araújo Lopes, PhD[1], Geovani Dantas Cassali, PhD[1], Ênio Ferreira, PhD[1], Emerson Soares Veloso[1], Elaine Amaral Leite, PhD[1], Fernão Castro Braga, PhD[1], Lucas Antônio Miranda Ferreira, PhD[1], Daniel Balvay, PhD[2], Anikitos Garofalakis, PhD[2], Mônica Cristina Oliveira, PhD[1], and Bertrand Tavitian, MD, PhD[2]

Abstract

Background. Ursolic acid (UA) is a triterpene found in different plant species, possessing antitumor activity, which may be a result of its antiangiogenic effect. However, UA has low water solubility, which limits its use because the bioavailability is impaired. To overcome this inconvenience, we developed long-circulating and pH-sensitive liposomes containing ursolic acid (SpHL-UA). We investigated the antiangiogenic effect of free UA and SpHL-UA in murine brain cancer and human breast tumor models by means of determination of the relative tumor volume, dynamic contrast-enhanced magnetic resonance imaging (DCE-MRI), and histopathological analysis. *Methods*. The animals were treated with dimethyl sulfoxide in 0.9% (w/v) NaCl, free UA, long-circulating and pH-sensitive liposomes without drug (SpHL), or SpHL-UA. The animals were submitted to each treatment by intraperitoneal injection for 5 days. The dose of free UA or SpHL-UA was equal to 23 mg/kg. *Results*. Tumor growth inhibition was not observed in human breast tumor–bearing animals. For murine gliosarcoma-bearing animals, a slight tumor growth inhibition was observed in the groups treated with free UA or SpHL-UA (9% and 15%, respectively). No significant change in any of the parameters evaluated by DCE-MRI for both experimental models could be observed. Nevertheless, the evaluation of the mean values of magnetic resonance parameters of human breast tumor–bearing animals showed evidence of a possible antiangiogenic effect induced by SpHL-UA. Histopathological analysis did not present significant change for any treatment. *Conclusion*. SpHL-UA did not show antiangiogenic activity in a gliosarcoma model and seemed to induce an antiangiogenic effect in the human breast tumor model.

Keywords

antiangiogenic, ursolic acid, dynamic contrast-enhanced magnetic resonance imaging, human breast tumor, murine brain cancer, long-circulating and pH-sensitive liposomes

Submitted Date: 4 October 2015; Revised Date: 1 December 2015; Accepted Date: 11 December 2015

Introduction

Ursolic acid (UA; 3β-hydroxy-urs-12-en-28-oic-acid) is a natural pentacyclic triterpenoid carboxylic acid derived from berries, leaves, flowers, and fruits of medicinal plants.[1-4] Several studies have demonstrated some pharmacological effects of UA, such as antioxidant, anti-inflammatory, antiproliferative, proapoptotic, antimetastatic, and antiangiogenic properties.[5-10] The investigation related to the use of UA as an anticancer agent has gained importance because of its action at various stages of tumor development and its low toxicity (LD_{50} = 7413 mg/kg for intravenous administration in mice).[11] Some studies have been performed dealing with

[1]Universidade Federal de Minas Gerais, Belo Horizonte, Minas Gerais, Brazil
[2]INSERM U970 , Université Paris Descartes, France

Corresponding Author:
Mônica Cristina Oliveira, Departamento de Produtos Farmacêuticos, Faculdade de Farmácia, Universidade Federal de Minas Gerais, Avenida Antônio Carlos, 6627, Belo Horizonte, Minas Gerais, Brazil.
Email: itabra2001@yahoo.com.br

the antiangiogenic action of UA. Sohn et al[12] examined the antiangiogenic activity of UA by using the chick embryo chorioallantoic membrane (CAM) assay. The presence of UA inhibited angiogenesis in a dose-dependent manner, and the dose required for half-maximal inhibition (ID_{50}) was 10 nmol. These authors also tested the inhibitory effect on the proliferation of bovine aortic endothelial cells. UA inhibited the proliferation of endothelial cells in a concentration-dependent manner (IC_{50} = 5 μM).[12] Cárdenas et al[13] have also demonstrated the antiangiogenic effect of UA in a CAM assay; 50 μmol of UA per CAM produced in vivo inhibition of angiogenesis in 100% of treated eggs. Furthermore, the UA effect on the migrating potential of endothelial cells was tested in the wound assay for bovine aortic endothelial cells. Concentrations of 1, 5, 10, and 15 μM were tested, and UA seemed to produce a dose-dependent inhibitory effect 24 hours after wounding. The effect of UA on capillary tube formation by endothelial cells was also assessed by an in vitro differentiation assay. The results showed that the minimal concentration of UA able to inhibit capillary tube formation by endothelial cell differentiation was 15 μM.[13] Kanjoormana and Kuttan[14] found that UA inhibits tumor-associated capillary formation in mice, induced by highly metastatic melanoma cells. Nontoxic concentrations of UA (10, 25, and 50 μM) reduced vessel growth from the rat aortic ring and inhibited proliferation, migration, and invasion of endothelial cells. Gelatin zymographic analysis also showed an inhibitory effect of UA on the protein expression of matrix metalloproteinases (MMPs) MMP-2 and MMP-9, which explains the inhibition of the invasion of cells. Although UA has shown antiangiogenic properties and low toxicity, its aqueous solubility is reduced, making its use as an antitumor agent difficult.[15,16] Thus, one of the major obstacles to pharmaceutical development is the limitation of the bioavailability and absorption of drugs. To overcome this limitation, several strategies have been proposed, such as the use of suitable drug delivery systems. Liposomes have gained attention as a carrier system for therapeutically active agents owing to their unique characteristics, including biocompatibility, biodegradability, lack of immune system activation, and capability to incorporate both hydrophilic and hydrophobic drugs.[17-19] In this context, our research group developed long-circulating and pH-sensitive liposomes containing UA (SpHL-UA). These liposomes are composed of dioleoylphosphatidylethanolamine (DOPE)/cholesteryl hemisuccinate (CHEMS)/distearoylphosphatidylethanolamine-polyethyleneglycol$_{2000}$ (DSPE-PEG$_{2000}$). In an acidic medium, such as that found in tumor sites and inside endosomes, CHEMS undergoes protonation, followed by the destabilization of liposomes and the release of UA in tumor sites or into the cytoplasm. Moreover, the long-circulating feature can prevent the recognition of liposomes by opsonins, thus reducing their clearance by cells of the mononuclear phagocyte system (MPS) and allowing an accumulation in tumor tissue.[20] In vitro experiments, carried out by our research group, showed that SpHL-UA is effective against human breast (MDA-MB-231) and prostate (LNCaP) cancer cell lines. Moreover, this formulation showed good stability after having been stored for 2 months at 4°C.[21] The use of UA in antitumor therapy is relatively recent, with few articles in the literature describing its antitumor activity in vivo and even fewer describing its antiangiogenic activity. Moreover, to date, there are no reports showing antiangiogenic treatment with UA in tumor models in which the tumor is a well-established and palpable nodule. To our knowledge, the in vivo studies of this kind of therapy have only described the chemopreventive effect of UA. Thus, this study is the first report concerning the investigation of the in vivo antiangiogenic treatment using UA in well-established tumor-bearing experimental animal models. It has been shown that UA is able to induce apoptosis in human breast cancer and glioma cell lines.[22,23] In this context, we investigated the antiangiogenic effect of free UA and SpHL-UA in murine brain cancer (9L cell line) and human breast tumor (MCF-7 cell line) models through evaluation by dynamic contrast-enhanced magnetic resonance imaging (DCE-MRI) and histopathology data. DCE-MRI is a technique that has been incorporated as a biomarker of drug efficacy in clinical trials of angiogenesis inhibitors.[24-26] DCE-MRI is a noninvasive quantitative method of investigating microvascular structure and function by tracking the pharmacokinetics of injected contrast agents as they pass through the tumor vasculature. The technique is sensitive to alterations in vascular permeability, extracellular extravascular and vascular volumes, and blood flow.[24,27,28]

Materials and Methods

Materials

DOPE and DSPE-PEG$_{2000}$ were supplied by Lipoid GmbH (Ludwigshafen, Germany). UA, CHEMS, phosphate saline buffer, and sodium hydroxide were obtained from Sigma Chemical Company (St Louis, MO, USA). Dulbecco's Modified Eagle's Medium (DMEM), fetal bovine serum (FBS), trypsin, and penicillin/streptomycin solution were purchased from Gibco Life Technologies (Carlsbad, USA). BD Matrigel was purchased from BD Biosciences (Mississauga, ON, Canada). Pellets of 17-β-estradiol (0.72 mg/pellet, 60-day release) were obtained from Innovative Research of America (Sarasota, FL, USA). Gadoterate dimeglumine (Dotarem) was purchased from Guerbet (Aulnay, France). All other chemicals and reagents used were of analytical grade. Human breast adenocarcinoma MCF-7 cell line transfected with luciferase gene and puromycin resistant was supplied by Dr Bertrand Tavitian (INSERM-U970, Paris, France). Rat gliosarcoma 9L cell line expressing the luciferase gene was supplied by Dr Alexandra Winkeler (CEA, Orsay, France). Female nude (NMRI-Foxn1nu/Foxn1nu) mice were purchased from Elevage Janvier (Le Genest-St-Isle, France).

Liposome Preparation

SpHL-UA were prepared as described by Lopes et al.[21] Briefly, 11.4 mL of DOPE 50 mM, 7.6 mL of CHEMS 50 mM, and 5 mL of DSPE-PEG_{2000} 10 mM, dissolved in chloroform, were transferred to a round bottom flask, amounting to a total lipid concentration of 20 mM (molar ratio of 5.7:3.8:0.5, respectively). UA equivalent at 0.1% (w/v) was added to the lipid solution. A lipid film was obtained by evaporating the chloroform under reduced pressure. Next, the lipid film was hydrated with 3.8 mL of NaOH 0.1M to promote the complete ionization of CHEMS molecules. Finally, 46.2 mL of phosphate-buffered saline (PBS), pH 7.4, was added. The obtained mixture was subjected to vigorous shaking in a vortex, producing multilamellar liposomes. The resulting multilamellar vesicles were calibrated using a single-stage high-pressure homogenizer, model APV 2000 (APV, Albertslund, Denmark) in recirculation mode. The homogenizer pressure was adjusted to 500 bar. The minimum volume of processed samples was 110 mL, and all homogenizations were carried out at room temperature. Each cycle was equal to the passage of the total volume of the sample through the homogenization chamber in a total of 12 cycles. Nonentrapped UA was separated by ultrafiltration using a polyethersulfone membrane (Millipore Pellicon XL device; Biomax, cut off 500 kDa; MA) connected to a tangential flow filtration system (Labscale; Millipore, MA, USA). The liposome dispersion (100 mL) was transferred to an initial container and pumped to the filtration membrane. Nonentrapped UA (permeated) was recovered in a flask, whereas purified SpHL-UA was returned to the initial container. This process was maintained until a concentrated SpHL-UA dispersion reached the final volume of 25 mL. After the cycle of ultrafiltration was completed, the permeated sample was taken, and the nonentrapped UA concentration was measured by high-performance liquid chromatography (HPLC; see the next section). In addition, the purified SpHL-UA was diluted with PBS buffer, pH 7.4, to the final volume of 50 mL, and the evaluation of drug entrapment was also performed by HPLC.

Liposome Characterization

SpHL-UA was characterized by drug entrapment quantification, size, polydispersity index, and ζ potential. The evaluation of drug entrapment was performed by HPLC before and after the purification of SpHL-UA, which was solubilized by adding methanol. The chromatographic apparatus consisted of a model 515 pump, a model 717 Plus autoinjector, and a model 2487 variable wavelength UV detector (Waters Instruments, USA) controlled by Empower software. Separations were performed using a 25 cm × 4 mm, 5-µm LiChrosorb, RP-18 column (Merck SA, Germany). The eluent system consisted of a 90:10 methanol/water mixture, and the flow rate was 1.5 mL/min. Samples (20 µL) were injected, and the eluate absorbance was monitored at 210 nm. The average diameter of vesicles was determined by photon correlation spectroscopy (PCS) at 25°C and at an angle of 90°. The ζ potential was evaluated by electrophoretic mobility determination at an angle of 90°. The size and ζ potential measurements were performed using the 3000HS Zetasizer equipment (Malvern Instruments, England). Each sample was diluted with PBS buffer solution.

Cell Culture

The rat gliosarcoma 9L cell line expressing the luciferase gene was maintained in DMEM supplemented with 10% FBS and 1% penicillin/streptomycin solution at 37°C in a 5% CO_2 atmosphere. The MCF-7 cell line transfected with the luciferase gene was maintained under the same conditions as those of the 9L cell line; however, the complete medium was supplemented with puromycin (2 µg/mL).

Animal Model

Female nude mice, 8 to 9 weeks old, were kept in plastic cages with free access to food and water in an area with a standardized light/dark cycle. All were held for a 1-week acclimatization period prior to beginning the experiments. All experiments were performed in accordance with both French law and US National Institutes of Health recommendations for animal care (Ethics Committee reference number 14-041).

MCF-7 Tumor Model

Once the cells reached 80% confluency, human breast cancer MCF-7 xenografts were established by subcutaneous inoculation of 10^6 cells in DMEM medium (in 1:1 volume ratio of DMEM and Matrigel) into the dorsal flank of nude mice. Cells were contained in a final volume of injection of 0.1 mL. Mice were implanted with a 17-β-estradiol pellet under their dorsal skin 24 hours before cell inoculation. Tumors were allowed to grow up to 30 days, approximately. After tumor growth, the animals were divided into 4 groups: animals treated with vehicle (10% dimethyl sulfoxide [DMSO] diluted in saline solution), free UA (UA dissolved in DMSO at a concentration of 10 mM and diluted in saline solution before use), SpHL, or SpHL-UA (n = 7 animals per group). Mice were submitted to each treatment by means of daily intraperitoneal injection for 5 days. The dose of free UA and SpHL-UA was equal to 23 mg/kg.

The 9L Tumor Model

After cells reached 80% confluency, nude mice were subcutaneously injected with an average of 10^6 tumor cells in DMEM medium into the dorsal flank. Cells were contained

in a final volume of injection of 0.1 mL. Tumors were allowed to grow up to 11 days, approximately. After tumor growth, the animals were divided into 4 groups and treated as described for the MCF-7 tumor model (n = 7 animals/group).

Evaluation of Antitumor Activity

Determination of Tumor Volume. Tumor volume (V) was determined by manually measuring 2 diameters with a caliper, length (a) and width (b), and calculated according to the following formula: $(a^2b)/2$, where $a < b$. The measurements were performed before and after the treatments described previously. The relative tumor volume (RTV) was calculated. For this, the first day on which the formulations were administered was considered day 0 (D0) of the study. As such, the formulations were administered from D0 to D4. Therefore, the antitumor activity was evaluated for a 5-day treatment period by calculating the RTV and the tumor growth inhibition ratio (IR), according to the following formulas:

$$\text{RTV} = \frac{\text{Tumor volume on D4}}{\text{Tumor volume on D0}}$$

and

$$\text{IR (\%)} = 1 - \frac{\text{Mean RTV of drug - treated group}}{\text{Mean RTV of control group}} \times 100.$$

DCE-MRI Evaluation. Nontoxic concentrations of UA (10, 25, and 50 μM) inhibit several key steps of the angiogenic process, such as inhibition of tumor-associated capillary formation and reduction in the levels of serum vascular endothelial growth factor (VEGF), NO, and proinflammatory cytokines.[14] VEGF plays an important role in angiogenesis initiation based on its ability to induce vasodilation via endothelial NO production and its endothelial cell permeability increasing effect.[29] We used DCE-MRI to analyze relevant parameters of vascular changes such as microvascular volume, vascular permeability, tissue blood flow, and rAUC (ratio between the area under the curve of the tumor and the area under the curve of the individual input artery) in the tumor models.

Experimental Design. After treatment, the mice were anesthetized with a 2.0% isoflurane/air mixture, followed by insertion of a catheter into the tail vein, which was attached to a syringe containing the Dotarem contrast agent. Next, the animals were placed on a cradle dedicated for mice under continuous exposure to 1% to 2% isoflurane. All DCE-MRI experiments were performed on a 1.5-T Siemens Symphony TIM MR system (Erlangen, Germany). The images were acquired with a 3D T1-weighted gradient echo sequence using a TR of 4.67 ms, a TE of 1.65 ms, and a flip angle of 12°. After obtaining the precontrast sequences, the paramagnetic contrast agent Dotarem diluted in 0.9% (w/v) NaCl solution was injected manually as a short bolus at a dose of 0.11 mmol/kg. Then, DCE-MRI sequences (0.7 mm thick slices, 320 × 280 mmfield of view, 380 × 300 matrix, 500 s scan duration) were acquired. The images were acquired sequentially with a high temporal resolution of 1.176 s per image and a spatial resolution of 312 × 312 μm. Dynamic data obtained were analyzed using MATLAB 7.2 software (R2006a, The Mathworks, Natick, MA, USA). All the fittings were based on the Levenberg-Marquardt regression method. Signal intensity measurements from 2 regions of interest (ROIs) were drawn for each examination: the first in the aorta lumen and the other in the solid tumor mass.[30] A rectangular ROI was positioned immediately above the renal artery and in the middle of the aorta to minimize partial volume effects (Figure 1A). The ROI was drawn on the raw DCE-MRI data on the slice and dynamic frame where the peak of the contrast enhancement was maximal within the defined ROI.

Pharmacokinetic Analysis. The aorta signal enhancement curve was used as the arterial input function with the pharmacokinetic model. The signal intensity versus time curves were converted into concentration equivalents assuming a near linear relationship between contrast agent concentration and signal enhancement.[31] Data analysis was performed using a bicompartmental model (Figure 2).[30,31] In this model, the tumor consists of a vascular compartment (Vb), an interstitial space (Ve) in which the contrast media diffuses, and a cellular compartment in which the contrast media does not diffuse. The tumor is then essentially a bicompartmental system with exchange between an interstitial compartment (Ve) and a vascular compartment (Vb) supplied by an arterial input (systemic blood arteries) and drained through a venous output. The analysis assumes that the volumes of the compartments are constant over the experimental time and that the mixing Please, eliminate the number "2".time within each compartment is short compared with the transfer of the tracer between compartments. In addition to tissue blood flow (F_T; mL/min/100 mL) and Vb (%), this model provides the product of permeability and surface area (PS; mL/min/100 mL) and Ve (%).

Histomorphometric Analysis of the Tumors. After DCE-MRI data acquisition, the animals were killed humanely by cervical spine dislocation, and tumors were removed and fixed in formalin (10% w/v in PBS, pH 7.4) for histopathological evaluation. Then, tissue samples were embedded in paraffin blocks, sectioned into a 3-μm thickness, placed onto glass slides, and stained by hematoxylin and eosin to perform histomorphometric evaluation. The images of cross-sections were obtained, and 10 fields per slide were examined using

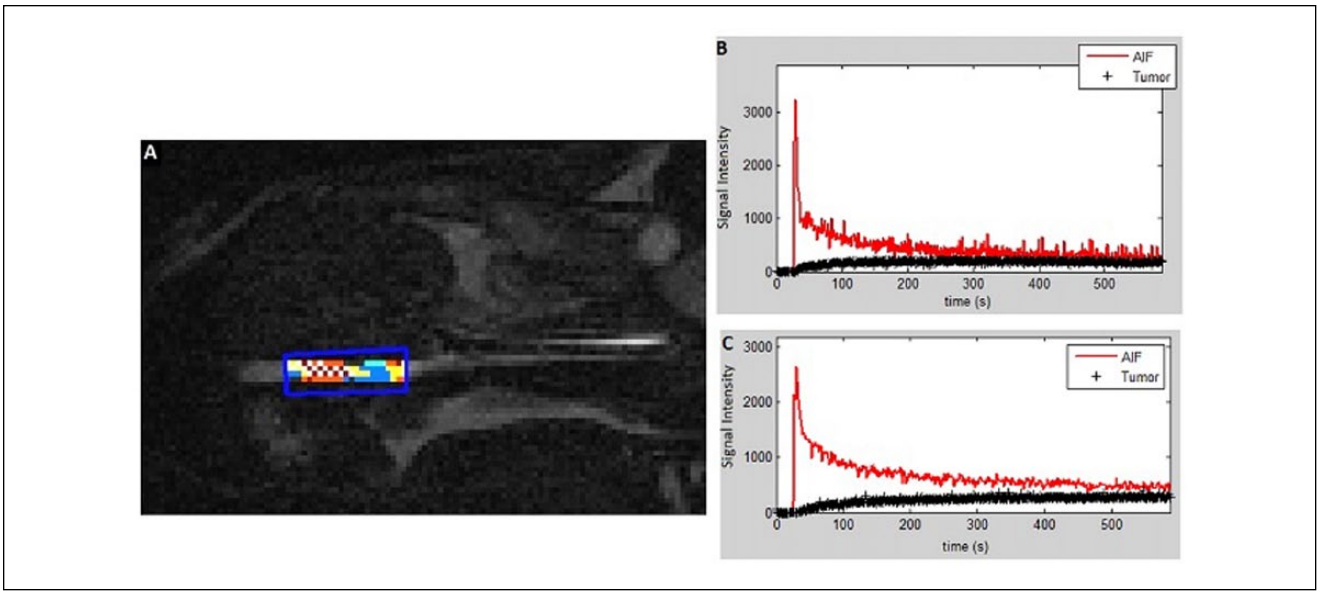

Figure 1. (A) ROI used to define AIF. (B) and (C) The AIF plot was defined by correlating the mean signal intensity value in each ROI against time.
Abbreviations: ROI, region of interest; AIF, arterial input function.

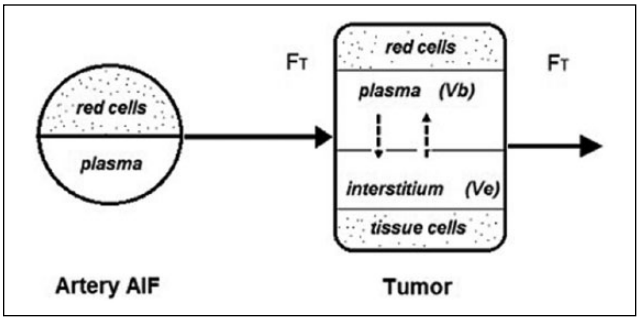

Figure 2. Two-compartment pharmacokinetic model: Blood transporting the contrast agent reaches the tumor tissue. Blood entering the capillaries contained in 1 voxel of tumor is characterized by the tumor blood flow (F_T). The tumor consists of a vascular compartment (Vb) and an interstitial space (Ve) supplied by an arterial input function (AIF; systemic blood arteries) and drained through a venous output. The contrast agent remains extracellular and does not diffuse into the tumor cells or red blood cells.

a 40× magnification in an optical microscope (final magnification = ×1000). The images were captured with a microcamera (Spot Insight Color; SPOT Imaging Solutions, Sterling Heights, MI, USA) attached to a microscope (Olympus BX-40; Olympus, Tokyo, Japan), and the Spot software, version 3.4.5, was used. Image analysis was performed using CorelDRAW (version 7.468; Microsoft Corporation, Redmond, USA, WA.[32] The percentages of necrotic area, viable neoplastic tissue, and inflammation were determined using a graticule of 25 dots. To assess the degree of neovascularization, histological sections were stained with Gomori's trichrome stain. Sections stained with hematoxylin and eosin were also captured—10 fields per slide using the 40× objective—followed by the quantification of vessels per field. The results were expressed as average vascular index (AVI). The assessment of cell proliferative activity was also performed. For this, the mitotic index (MI) was calculated in sections stained with hematoxylin and eosin by performing the mitotic count in 10 random fields. This determination was also made using a 40× objective.

Statistical Analysis

The normality and homogeneity of the variance analysis were performed using the D'Agostino-Pearson and Bartlett's tests, respectively. Differences among the experimental groups were tested using the 1-way ANOVA, followed by the Tukey's test, with P values of $<.05$ regarded as significant (Graphpad Prism 5.0, Graphpad Software Inc, San Diego, CA, USA).

Results

SpHL-UA Characterization

The average diameters of the vesicles of SpHL-UA and UA entrapment were equal to 182.7 ± 8.0 nm and 0.77 ± 0.02 mg/mL, respectively. The polydispersity index was equal to 0.60 ± 0.07, and approximately 90% of the vesicles had a mean diameter of ≤300 nm. SpHL-UA exhibited a ζ potential value near

Table 1. RTV in Human Breast Tumor–Bearing Nude Mice After Treatment.[a]

	Treatment			
	DMSO in saline solution	Free UA	SpHL	SpHL-UA
RTV (mean ± SEM)	0.58 ± 0.14	0.79 ± 0.24	0.68 ± 0.14	1.22 ± 0.20

Abbreviations: RTV, relative tumor volume; DMSO, dimethyl sulfoxide; UA, ursolic acid; SpHL, long-circulating and pH-sensitive liposomes; SpHL-UA, long-circulating pH-sensitive liposomes containing UA.
[a]Values are given as mean ± standard error of the mean (SEM). Number of animals per group: n = 3, DMSO in saline solution; n = 3, free UA; n = 4, SpHL; n = 5, SpHL-UA.

Table 2. Evaluation of DCE-MRI Quantitative Parameters in Human Breast Tumor–Bearing Nude Mice After Treatment.[a]

	Treatment			
Parameter	DMSO in Saline Solution	Free UA	SpHL	SpHL-UA
F_T (mL/min/100 mL)	31.93 ± 9.66	20.79 ± 6.15	33.14 ± 12.71	11.69 ± 1.73
Vb (%)	28.57 ± 12.07	23.76 ± 5.37	23.68 ± 3.63	10.91 ± 4.36
PS (mL/min/100 mL)	9.35 ± 2.84	5.17 ± 1.23	13.59 ± 7.08	6.09 ± 2.84
Ve (%)	33.84 ± 11.38	31.49 ± 6.75	30.62 ± 9.05	39.72 ± 13.60
rAUC	0.53 ± 0.18	0.38 ± 0.08	0.45 ± 0.14	0.28 ± 0.05

Abbreviations: DCE-MRI, dynamic contrast-enhanced magnetic resonance imaging; DMSO, dimethyl sulfoxide; UA, ursolic acid; SpHL, long-circulating and pH-sensitive liposomes; SpHL-UA, long-circulating pH-sensitive liposomes containing UA; F_T, tissue blood flow; Vb, blood volume fraction; PS, product of permeability and surface area; Ve, extracapillary and extracellular (interstitial) volume fraction; rAUC, relative area under the enhancing curve.
[a]Values are given as mean ± standard error of the mean. Number of animals per group: n =3, DMSO in saline solution; n = 3, free UA; n = 4, SpHL; n = 5, SpHL-UA.

neutrality (0.3 ± 1.6 mV). Long-circulating and pH-sensitive liposomes without drug (SpHL) showed mean diameter, polydispersity index, and ζ potential values equal to 105.6 ± 3.1 nm, 0.23 ± 0.03, and 0.6 ± 5.4 mV, respectively. These findings are similar to those described previously by Lopes et al.[21]

Evaluation of the Antitumor Activity

The antitumor activity of the SpHL-UA and free UA treatments was assessed at a dose of 23 mg/kg, administered daily for 5 days in murine brain tumor or human breast tumor–bearing nude mice. The animals selected to have their data analyzed statistically were those who had a tumor volume within the range mean ± SD.

MCF-7 Tumor-Bearing Mice

Antitumor activity of SpHL-UA and free UA were initially evaluated by the tumor volume variation analysis over time. The results are described in Table 1. Mice treated with free UA or SpHL-UA showed no significant difference when compared with their control groups. Moreover, the group treated with SpHL-UA also presented no statistical difference when compared with the group treated with free UA. Tumor growth inhibition was not observed in animals treated with free UA or SpHL-UA.

Next, we used DCE-MRI as a biomarker of UA efficacy as an angiogenesis inhibitor. The results of tissue blood flow (FT), blood volume fraction (Vb), PS, extracapillary and extracellular (interstitial) volume fraction (Ve), and relative area under the enhancing curve (rAUC) analyzed are reported in Table 2. The results obtained showed no significant difference between the groups treated with free UA or SpHL-UA and their respective controls. Also, no significant difference was observed between free-UA- and SpHL-UA-treated groups. However, the mean values tend to be different when analyzing certain parameters for the groups in question. Furthermore, if the mean data are taken together, they suggest a possible effect of the analyzed drug. First, an average FT parameter reduction for the groups treated with UA was noted. The group treated with SpHL-UA presented an even greater reduction in the mean value when compared with its control group. Concerning this parameter, 40.0% of the animals treated with SpHL-UA and 33.3% of the animals treated with free UA presented with FT values below the mean of their respective groups. The mean value of Vb for the group treated with SpHL-UA was also reduced with respect to control and free-UA groups. Furthermore, the mean values of the PS parameter decreased to approximately half for the groups treated with free UA or SpHL-UA in relation to their control groups. Where this parameter was concerned, 80.0% of the animals treated with SpHL-UA showed values below the mean, and 66.7% of the animals treated with free UA presented with lower values than the mean value of its respective group. The average value of Ve for the group treated with SpHL-UA

Table 3. Morphometric Parameters Observed in Human Breast Tumor–Bearing Nude Mice After Treatment.[a]

	Parameter				
Treatment	Inflammation (%)	Necrosis (%)	Neoplasia (%)	AVI	MI
DMSO in saline solution	1.87 ± 0.81	7.20 ± 4.33	90.93 ± 4.90	1.40 ± 0.20	3.20 ± 0.36
Free UA	1.60 ± 0.46	18.13 ± 2.53	88.00 ± 5.22	1.43 ± 0.71	4.33 ± 0.77
SpHL	2.00 ± 1.22	24.33 ± 7.02	73.40 ± 7.38	1.45 ± 0.30	4.35 ± 0.88
SpHL-UA	2.32 ± 1.12	12.88 ± 3.50	84.80 ± 4.50	1.30 ± 0.25	4.38 ± 0.44

Abbreviations: AVI, average vascular index; MI, mitotic index; DMSO, dimethyl sulfoxide; UA, ursolic acid; SpHL, long-circulating and pH-sensitive liposomes; SpHL-UA, long-circulating pH-sensitive liposomes containing UA.
[a]Values are given as mean ± standard error of the mean. Number of animals per group: n = 3, DMSO in saline solution; n = 3, free UA; n = 4, SpHL; n = 5, SpHL-UA.

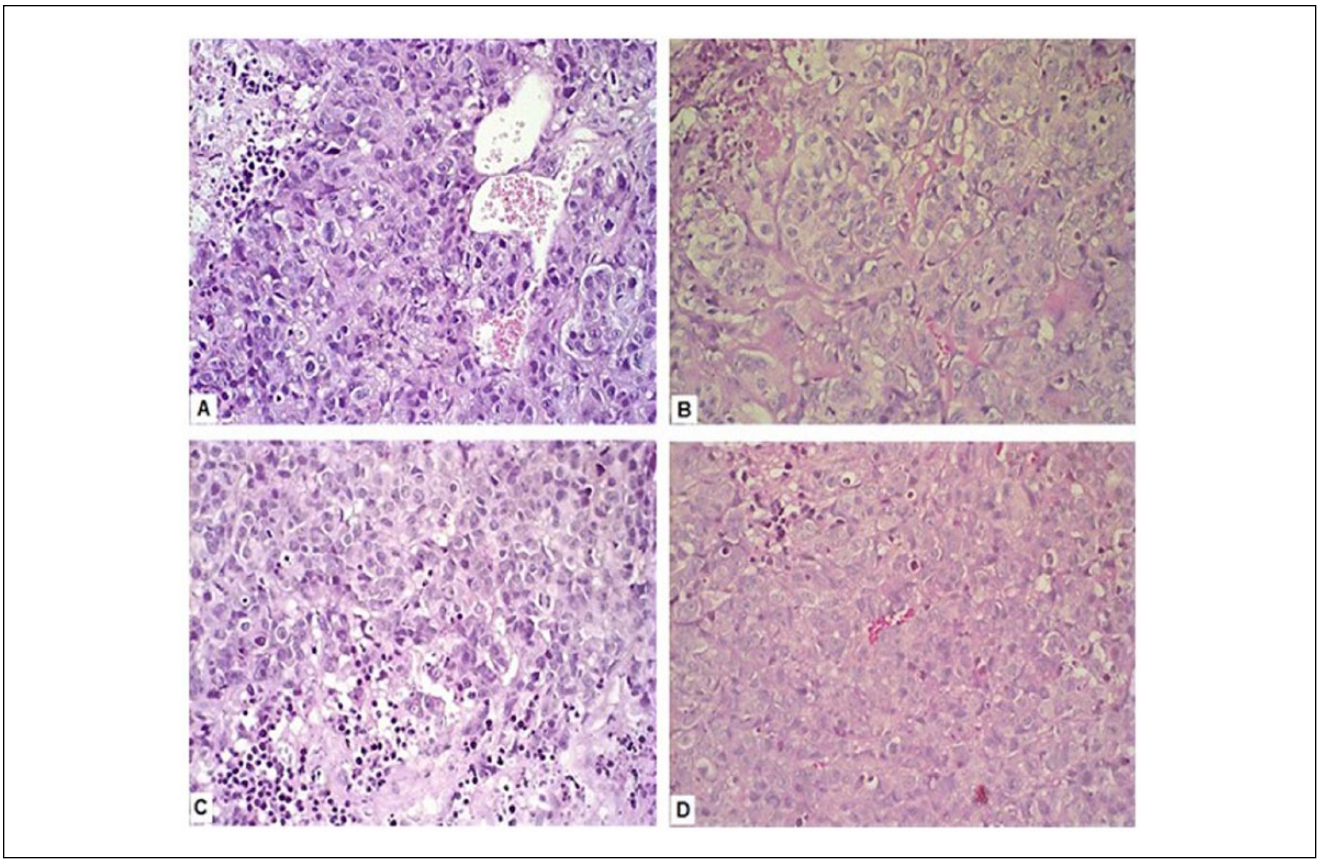

Figure 3. Photomicrographs of tumor of human breast tumor–bearing nude mice after treatment. (A) DMSO solution in saline, (B) free UA, (C) SpHL, and (D) SpHL-UA (hematoxylin and eosin staining).
Abbreviations: DMSO, dimethyl sulfoxide; UA, ursolic acid; SpHL, long-circulating and pH-sensitive liposomes; SpHL-UA, long-circulating and pH-sensitive liposomes containing UA.

showed a small increase in relation to its control group. The mean values for the last parameter shown in Table 2, rAUC, were reduced for the groups treated with free or encapsulated UA in liposomes when compared with their control groups. The average value of this parameter was also lower in the group treated with SpHL-UA than in the group treated with free UA. In this case, 60.0% of the animals treated with SpHL-UA showed rAUC values below the mean, and 33.3% of the animals treated with free UA showed values below the average of the group.

Histomorphometric analyses were also performed to confirm the results obtained by DCE-MRI, and the results are shown in Table 3. Tumor tissue of all groups showed inflammation, necrosis, and neoplasia areas. Tissue samples of all groups showed a predominance of neoplasia areas with a low percentage of inflammatory cells and few regions

Table 4. RTV in 9L Tumor-Bearing Nude Mice After Treatment.[a]

	Treatment			
	DMSO in Saline Solution	Free UA	SpHL	SpHL-UA
RTV (mean ± SEM)	2.16 ± 0.55	1.97 ± 0.26	1.50 ± 0.16	1.33 ± 0.27

Abbreviations: RTV, relative tumor volume; DMSO, dimethyl sulfoxide; UA, ursolic acid; SpHL, long-circulating and pH-sensitive liposomes; SpHL-UA, long-circulating and pH-sensitive liposomes containing UA.
[a]Values are given as mean ± standard error of the mean (SEM). Number of animals per group: n = 6, DMSO in saline solution; n = 5, free UA; n = 5, SpHL; n = 4, SpHL-UA.

Table 5. Evaluation of DCE-MRI Quantitative Parameters in 9L Tumor-Bearing Nude Mice After Treatment.[a]

	Treatment			
Parameter	DMSO in Saline Solution	Free UA	SpHL	SpHL-UA
F_T (mL/min/100 mL)	35.17 ± 2.95	40.25 ± 12.21	45.27 ± 5.04	52.48 ± 21.82
Vb (%)	33.09 ± 5.21	31.18 ± 6.38	28.58 ± 3.45	37.45 ± 11.46
PS (mL/min/100 mL)	6.71 ± 0.73	5.98 ± 1.54	9.23 ± 1.19	10.19 ± 2.71
Ve (%)	29.73 ± 7.86	20.44 ± 2.79	25.11 ± 2.79	27.66 ± 6.31
rAUC	0.53 ± 0.07	0.45 ± 0.09	0.53 ± 0.01	0.64 ± 0.19

Abbreviations: DCE-MRI, dynamic contrast-enhanced magnetic resonance imaging; DMSO, dimethyl sulfoxide; UA, ursolic acid; SpHL, long-circulating and pH-sensitive liposomes; SpHL-UA, long-circulating and pH-sensitive liposomes containing UA; F_T, tissue blood flow; Vb, blood volume fraction; PS, product of permeability and surface area; Ve, extracapillary and extracellular (interstitial) volume fraction; rAUC, relative area under the enhancing curve.
[a]Values are given as mean ± standard error of the mean. Number of animals per group: n = 4, DMSO in saline solution; n = 5, free UA; n = 3, SpHL; n = 3, SpHL-UA.

of necrosis. No significant difference in these parameters was noted among the groups analyzed. The degree of neovascularization was also evaluated, and the AVI for the groups assessed did not reflect significant changes after treatment with free UA or SpHL-UA. Finally, the proliferative activity of tumor cells was assessed by determining the MI. Also, in this evaluation, no statistical difference was observed following treatment of mice with free UA or SpHL-UA when compared with their respective control groups or between UA- and SpHL-UA-treatment groups. Representative histological sections stained by hematoxylin and eosin are shown in Figure 3.

The 9L Tumor-Bearing Mice

Antitumor activity of SpHL-UA for 9L tumor-bearing mice was also initially evaluated by tumor volume variation analysis over time. The tumor volume increased for all treated groups (Table 4). No significant difference was observed for RTV in mice treated with SpHL-UA or free UA as compared with their control groups. Also, no significant difference was observed in mice treated with SpHL-UA as compared with mice treated with free UA. Ultimately, a slight growth inhibition was observed in the groups treated with free UA and SpHL-UA (9% and 15%, respectively).

The antiangiogenic effect of UA was evaluated by DCE-MRI. The analyzed parameter results are shown in Table 5. As in the MCF-7 model, no significant difference was observed between the free-UA- or the SpHL-UA-treated groups and their respective controls. Also, no significant difference was noted between the groups treated with free UA or SpHL-UA.

Tissue morphometric analysis was also performed, and the results are shown in Table 6. The tumor samples of all groups evaluated showed areas of inflammation, necrosis, and neoplasia. The tumor tissue samples of all treated groups showed a low percentage of inflammatory cells and few areas of necrosis, with no significant difference in these parameters between the groups analyzed. Regarding the degree of neovascularization, the AVI did not show significant changes after treatment with free UA or SpHL-UA. In addition, the proliferative activity of tumor cells, expressed by MI, showed no statistical difference following treatment with free UA or SpHL-UA when compared with their respective control groups as well as when the 2 treated groups were themselves compared. Figure 4 illustrates representative histological sections stained by hematoxylin and eosin after different treatments.

Discussion

Angiogenesis inhibitors are a relatively new class of anticancer drugs that inhibit the growth of newly formed vessels. These new blood vessels are recruited by tumors that typically have a critical value exceeding 1 to 2 mm.[3,25,33] UA is a promising anticancer agent that shows antiangiogenic effect

Table 6. Morphometric Parameters Observed in 9L Tumor-Bearing Nude Mice After Treatment.[a]

	Parameter				
Treatment	Inflammation (%)	Necrosis (%)	Neoplasia (%)	AVI	MI
DMSO in saline solution	1.33 ± 0.56	12.53 ± 3.27	86.13 ± 3.16	3.98 ± 0.77	1.43 ± 0.35
Free UA	1.28 ± 0.34	5.36 ± 1.71	93.44 ± 1.87	2.60 ± 0.67	1.48 ± 0.25
SpHL	1.30 ± 0.64	18.30 ± 5.91	80.40 ± 6.48	2.85 ± 0.66	1.88 ± 0.39
SpHL-UA	0.40 ± 0.40	13.50 ± 3.98	86.10 ± 4.31	2.35 ± 0.30	0.78 ± 0.06

Abbreviations: AVI, average vascular index; MI, mitotic index; DMSO, dimethyl sulfoxide; UA, ursolic acid; SpHL, long-circulating and pH-sensitive liposomes; SpHL-UA, long-circulating and pH-sensitive liposomes containing UA.
[a]Values are given as mean ± standard error of the mean. Number of animals/group: n = 6, DMSO in saline solution; n = 5, free UA; n = 4, SpHL; n = 4, SpHL-UA.

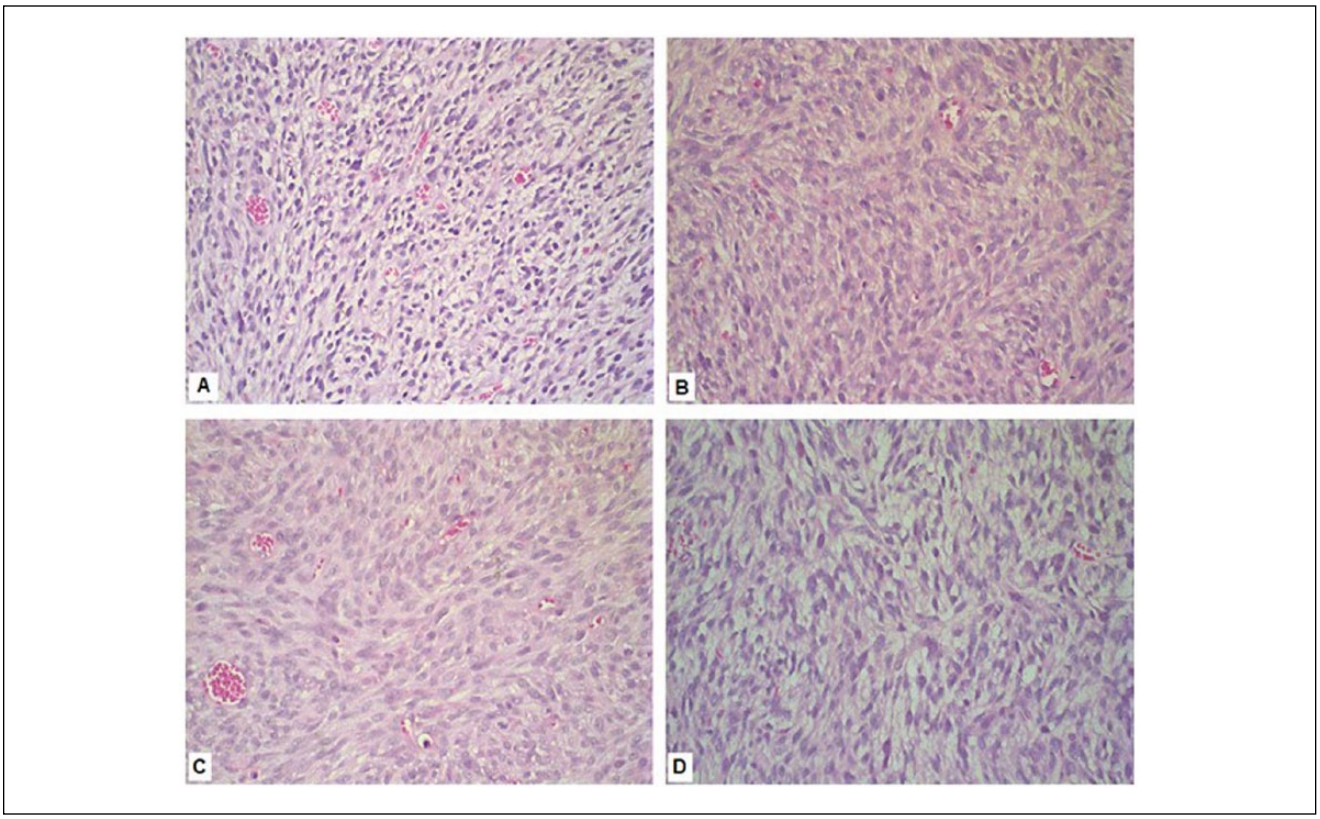

Figure 4. Photomicrographs of tumor of 9L tumor-bearing nude mice after treatment: (A) DMSO solution in saline, (B) free UA, (C) SpHL, and (D) SpHL-UA (hematoxylin and eosin staining).
Abbreviations: DMSO, dimethyl sulfoxide; UA, ursolic acid; SpHL, long-circulating and pH-sensitive liposomes; SpHL-UA, long-circulating and pH-sensitive liposomes containing UA.

at nontoxic concentrations. This effect could be the result of the reduction in the production of VEGF, MMP-2, MMP-9, and NO, whose levels are related to the tumor-directed capillary formation and endothelial cell proliferation, migration, and invasion. One major problem associated with its administration is its low aqueous solubility, which leads to a low bioavailability in vivo and hence restricts its effectiveness. To overcome this, SpHL-UA was developed by our research group, and its antiangiogenic activity was evaluated in human breast adenocarcinoma and murine gliosarcoma-bearing experimental animal models.

SpHL-UA obtained for this study had an adequate mean diameter (182 nm) for anticancer treatment by the intraperitoneal route. The liposome size can vary from very small (0.025 μm) to large (2.5 μm) vesicles. Vesicle size is a critical parameter that determines the fraction of liposomes cleared by the organs of the MPS.[34] Another factor related to liposome uptake by the MPS is the presence of polymer

molecules, such as PEG, on the liposome surface. PEG molecules form a protective hydrophilic layer on the surface of liposomes, which prevents their aggregation and interaction with the blood components, consequently extending their blood circulation time.[35,36] Therefore, SpHL-UA can lead to a higher drug concentration on the active site because of its additional long-circulating feature. In addition, SpHL-UA can undergo destabilization when submitted to an acidic environment at the endosomal stage, thereby preventing drug degradation at the lysosomal level and promoting the release of UA into the cytoplasm.[20,34] Leite et al[37] evaluated the antitumor activity of SpHL containing cisplatin (SpHL-CDDP) after intravenous administration in solid Ehrlich tumor–bearing mice and compared it with the activity of free CDDP and long-circulating and non-pH-sensitive liposomes containing CDDP (NSpHL-CDDP). The doses assessed were 8 mg/kg for free CDDP and 8 or 16 mg/kg for SpHL-CDDP and NSpHL-CDDP, administered once weekly over a 3-week period. A significant reduction in the tumor volume and a higher tumor growth IR was observed after SpHL-CDDP therapy (16 mg/kg) when compared with free CDDP treatment. Furthermore, complete remission of tumor was detected in 18.2% of the mice treated with SpHL-CDDP at a dose of 16 mg/kg. As such, the administration of SpHL-CDDP (16 mg/kg), as compared with free CDDP and NSpHL-CDDP (16 mg/kg), led to a decrease in the area of necrosis and in the percentage of positive CDC-47 tumor cells. A significant reduction in the VEGF serum level was also observed after SpHL-CDDP (16 mg/kg) treatment when compared with free-CDDP treatment.[37] De Barros et al[38] evaluated the ability of SpHL containing a bombesin derivative labeled with technetium-99 m (^{99m}Tc-BBN$_{(7–14)}$) and long-circulating non-pH sensitive liposomes (nSpHL), also containing the radiotracer, to identify Ehrlich tumors in a mouse model. Biodistribution studies were performed in Ehrlich tumor–bearing mice to compare the ability of SpHL and nSpHL to deliver ^{99m}Tc-BBN$_{(7–14)}$ to the tumor site. Results showed higher tumor uptake (2-fold) when pH-sensitive liposomes were used, suggesting that these vesicles can facilitate access to the tumor by releasing the diagnostic agent into the ideal area. A higher tumor-to-muscle ratio was obtained when pH-sensitive liposomes were used when compared with a non-pH-sensitive formulation. Scintigraphic images were also obtained, and animals treated with pH-sensitive liposomes showed evident tumor uptake, corroborating the biodistribution data. The authors suggested that pH-sensitive liposomes are able to deliver the radiolabeled bombesin analog more efficiently.[38]

The use of UA in antitumor therapy in preclinical experiments can be considered a recent development. A small number of in vivo studies in the literature describe its cytotoxic activity, and even fewer describe its antiangiogenic activity. The treatment schedule used in this study was based on that carried out by Kanjoormana and Kuttan.[14] This group of researchers evaluated the effect of UA on capillary formation caused by the presence of melanoma (strain B16F-10), after intraperitoneal injection for 5 consecutive days at a dose of 23 mg/kg in C57BL/6mice. A significant reduction in the number of tumor-associated capillaries was observed in the group treated with UA when compared with the control group (42.0% of reduction). It is interesting to note that unlike cytotoxic therapy, the angiogenesis inhibitors are most effective when administered as a continuous treatment regimen at a low dose.[14,39-42] Thus, in our study, a treatment regimen consisting of continuous administration of free UA or SpHL-UA was used at a dose equal to 23 mg/kg.

The first technique used was the analysis of the variation of tumor volume before and after treatment, which allows the observation of initial tumor volume reduction or stabilization. There was no statistical difference between the groups treated with UA and their respective control groups or between the group treated with SpHL-UA and the free UA group for both tested lines. The IR was also calculated from RTV data. Animals inoculated with the MCF-7 line exhibited no inhibition of tumor growth after treatment with free UA or SpHL-UA, and those inoculated with the 9L cell line showed only a slight inhibition of growth (free UA, IR = 9%; SpHL-UA, IR = 15%). Next, we used DCE-MRI to evaluate quantitative hemodynamic parameters, such as F_T, PS, Vb, Ve, and rAUC. Results of DCE-MRI parameters for human breast adenocarcinoma tumor–bearing animals were not statistically different for the analyzed groups. However, when the mean values obtained for the analyzed parameters are jointly evaluated, there is a tendency of a possible UA antiangiogenic effect. The reduction in F_T average for the groups treated with UA is probably a result of impaired delivery of nutrients and oxygen to the tumor.[43] Liposome-encapsulated UA may have led to a better cellular drug uptake, causing a more pronounced effect in this group. It is important to note that 40.0% and 33.3% of the animals treated with SpHL-UA or free UA, respectively, showed average values of F_T below the mean value of the respective group. The most pronounced reduction in Vb mean value in the SpHL-UA-treated group is probably a result of the decrease in perfusion (also more pronounced) observed in this group. The reduction in PS mean values in the groups treated with free UA or SpHL-UA may be because of the more mature nature of the vessels, the presence of better connections between adjacent endothelial cells, an increase in the proportion of vessels covered by perivascular cells (pericytes and vascular smooth muscle cells), and a closer association between perivascular and endothelial cells.[43-45] In this case, it is important to highlight that 80.0% of SpHL-UA-treated animals and 66.7% of free-UA-treated animals had PS values below the mean value of their respective groups. Most biologically active drugs do not cause changes

in Ve, although there are significant changes in other parameters.[46] Finally, in agreement with the results obtained, there is a reduction in mean values of SpHL-UA- or free-UA-treated groups in relation to their control groups. These results suggest a decrease in the contrast agent concentration in the tumor region, probably because of the reduced perfusion and permeability parameters. Regarding this parameter, 60.0% of SpHL-UA-treated animals and 33.3% of free-UA-treated animals showed values below the mean of their respective groups. The evaluation of the same parameters in gliosarcoma-bearing mice resulted in no statistical difference between the groups analyzed and did not show any trend as observed for the animals inoculated with the MCF-7 cell line. Finally, histopathological analyses were performed to evaluate inflammation, necrosis, and neoplasia areas, beyond the degree of neovascularization and proliferation activity of tumor cells. In both tumor models, there were no statistical differences in the evaluated parameters between interest groups.

To our knowledge, our study is the first to evaluate the in vivo antiangiogenic treatment using UA in breast adenocarcinoma or gliosarcoma-bearing experimental animal models. Substantial evidence of UA antiangiogenic effect was observed in the MCF-7 tumor model by the adopted treatment regimen. However, for the second one, the same signs were not detected. We suggest that the lack of antiangiogenic effect using free UA or SpHL-UA treatments in animals inoculated with the 9L cell line may be related to the experimental animal models where the tumor was presented as a well-established and palpable nodule. In the study on which our research was based, the therapy began shortly after the injection of tumor cells in animals. In our experiments, we simulated a real situation, such as the treatment of an established tumor and not a chemopreventive treatment. The latter model, wherein the drug is administered before the tumor challenge, is a prophylactic treatment model and is not considered realistic. This type of treatment has been described as a way to extend antitumor drug activity. This tumor model has been reported as a supersensitive model to the subsequent chemotherapy.[47,48] Another explanation for the absence of the expected results in the gliosarcoma tumor model and the presence of evidence of a possible antiangiogenic effect in the breast adenocarcinoma tumor model may be related to the kinetics of the antiangiogenic effect. The achievement of this effect may occur weeks or months after the treatments.[49-51]

Conclusion

UA has aroused interest in therapy cancer because of its activities at various stages of tumor development and its low toxicity. This study is the first report of in vivo treatment using UA encapsulated in liposomes (SpHL-UA) to evaluate its antiangiogenic activity. It is also the first study describing the treatment with free UA or SpHL-UA using well-established tumor-bearing experimental animal models. The continuous administration of SpHL-UA for 5 days at a dose equal to 23 mg/kg did not result in an antiangiogenic effect in an experimental animal model of murine gliosarcoma (9L cell line) but showed strong indications of a possible effect on the human breast adenocarcinoma experimental model (MCF-7 cell line). Further studies are needed to evaluate the antitumor efficacy of formulations containing UA for a period of treatment up to 5 days and the use of higher doses as well as to monitor tumor progress during a prolonged time period.

Authors' Note

All experiments were performed in accordance with both French law and US National Institutes of Health recommendations for animal care (Ethics Committee reference number 14-041).

Declaration of Conflicting Interests

The author(s) declared no potential conflicts of interest with respect to the research, authorship, and/or publication of this article.

Funding

The author(s) disclosed receipt of the following financial support for the research, authorship, and/or publication of this article: The authors would like to thank Fundação de Amparo à Pesquisa do Estado de Minas Gerais (FAPEMIG) for financial support (Grant Number CDS-PPM-00525-11, Rede-40/11, PPM-00477-13). The authors also thank Coordenação de Aperfeiçoamento de Pessoal de Nível Superior-CAPES, Brazil, for supporting this project with a scholarship (Grant Number CAPES-7742009).

References

1. Liu J. Pharmacology of oleanolic acid and ursolic acid. *J Ethnopharmacol*. 1995;49:57-68.
2. Ikeda Y, Murakami A, Ohigashi H. Ursolic acid: an anti- and pro-inflammatory triterpenoid. *Mol Nutr Food Res*. 2008;52:26-42.
3. Shanmugam MK, Nguyen AH, Kumar AP, Tan BK, Sethi G. Targeted inhibition of tumor proliferation, survival, and metastasis by pentacyclic triterpenoids: potential role in prevention and therapy of cancer. *Cancer Lett*. 2012;320:158-170.
4. Wu B, Wang X, Chi ZF, et al. Ursolic acid-induced apoptosis in K562 cells involving upregulation of PTEN gene expression and inactivation of the PI3K/Akt pathway. *Arch Pharm Res*. 2012;35:543-548.
5. Yan SL, Huang CY, Wu ST, Yin MC. Oleanolic acid and ursolic acid induce apoptosis in four human liver cancer cell lines. *Toxicol in Vitro*. 2010;24:842-848.
6. Yeh CT, Wu CH, Yen GC. Ursolic acid, a naturally occurring triterpenoid, suppresses migration and invasion of human breast cancer cells by modulating c-Jun N-terminal kinase, Akt and mammalian target of rapamycin signaling. *Mol Nutr Food Res*. 2010;54:1285-1295.

7. Zheng QY, Jin FS, Yao C, Zhang T, Zhang GH, Ai X. Ursolic acid-induced AMP-activated protein kinase (AMPK) activation contributes to growth inhibition and apoptosis in human bladder cancer T24 cells. *Biochem Biophys Res Commun*. 2012;419:741-747.
8. Yadav VR, Prasad S, Sung B, Kannappan R, Aggarwal BB. Targeting inflammatory pathways by triterpenoids for prevention and treatment of cancer. *Toxins*. 2010;2:2428-2466.
9. Harmand PO, Duval R, Delage C, Simon A. Ursolic acid induces apoptosis through mitochondrial intrinsic pathway and caspase-3 activation in M4Beu melanoma cells. *Int J Cancer*. 2005;114:1-11.
10. Bonaccorsi I, Altieri F, Sciamanna I, et al. Endogenous reverse transcriptase as a mediator of ursolic acid's anti-proliferative and differentiating effects in human cancer cell lines. *Cancer Lett*. 2008;263:130-139.
11. Xie J, Bai Y, Yi Y, Yang G, Zhang C. Freeze-dried lecithin nanometer powder injection of ursolic acid and its preparation method. http://patentscope.wipo.int/search/en/detail.jsf?docId=WO2004045619&recNum=132&docAn=CN2003000969&queryString=%28FP/bcl-2%29%2520&maxRec=219. Accessed November 22, 2013.
12. Sohn KH, Lee HY, Chung HY, Young HS, Yi SY, Kim KW. Anti-angiogenic activity of triterpene acids. *Cancer Lett*. 1995;94:213-218.
13. Cárdenas C, Quesada AR, Medina MA. Effects of ursolic acid on different steps of the angiogenic process. *Biochem Biophys Res Commun*. 2004;320:402-408.
14. Kanjoormana M, Kuttan G. Antiangiogenic activity of ursolic acid. *Integr Cancer Ther*. 2010;9:224-235.
15. Jin IJ, Ko YI, Kim YM, Han SK. Solubilization of oleanolic acid and ursolic acid by cosolvency. *Arch Pharm Res*. 1997;20:269-274.
16. Zhou XJ, Hu XM, Yi YM, Wan J. Preparation and body distribution of freeze-dried powder of ursolic acid phospholipid nanoparticles. *Drug Dev Ind Pharm*. 2009;35:305-310.
17. Torchilin VP. Recent advances with liposomes as pharmaceutical carriers. *Nat Rev Drug Discov*. 2005;4:145-160.
18. Laouini A, Jaafar-Maalej C, Limayem-Blouza I, Sfar S, Charcosset C, Fessi H. Preparation, characterization and applications of liposomes: state of the art. *J Colloid Sci Biotechnol*. 2012;1:147-168.
19. Perche F, Torchilin VP. Recent trends in multifunctional liposomal nanocarriers for enhanced tumor targeting. *J Drug Deliv*. 2013;2013:705265.
20. Simões S, Moreira JN, Fonseca C, Düzgüneş N, de Lima MC. On the formulation of pH-sensitive liposomes with long circulation times. *Adv Drug Deliv Rev*. 2004;56:947-965.
21. Lopes SCA, Novais MVM, Teixeira CS, et al. Preparation, physicochemical characterization, and cell viability evaluation of long-circulating and pH-sensitive liposomes containing ursolic acid. *Biomed Res Int*. 2013;2013:467147.
22. Wang JS, Ren TN, Xi T. Ursolic acid induces apoptosis by suppressing the expression of FoxM1 in MCF-7 human breast cancer cells. *Med Oncol*. 2012;29:10-15.
23. Wang J, Li Y, Wang X, Jiang C. Ursolic acid inhibits proliferation and induces apoptosis in human glioblastoma cell lines U251 by suppressing TGF-beta1/miR-21/PDCD4 pathway. *Basic Clin Pharmacol Toxicol*. 2012;111:106-112.
24. O'Connor JP, Jackson A, Parker GJ, Jayson GC. DCE-MRI biomarkers in the clinical evaluation of antiangiogenic and vascular disrupting agents. *Br J Cancer*. 2007;96:189-195.
25. Ehling J, Lammers T, Kiessling F. Non-invasive imaging for studying anti-angiogenic therapy effects. *Thromb Haemost*. 2013;109:375-390.
26. Moestue SA, Huuse EM, Lindholm EM, et al. Low-molecular contrast agent dynamic contrast-enhanced (DCE)-MRI and diffusion-weighted (DW)-MRI in early assessment of bevacizumab treatment in breast cancer xenografts. *J Magn Reson Imaging*. 2013;38:1043-1053.
27. Pradel C, Siauve N, Bruneteau G, et al. Reduced capillary perfusion and permeability in human tumour xenografts treated with the VEGF signalling inhibitor ZD4190: an in vivo assessment using dynamic MR imaging and macromolecular contrast media. *Magn Reson Imaging*. 2003;21:845-851.
28. Hundt W, Steinbach S, O'Connell-Rodwell CE, Mayer D, Burbelko M, Guccione S. In vivo monitoring of antiangiogenic therapy by magnetic resonance and bioluminescence imaging in an M21 tumor model through activation of an hsp70 promoter–luciferase reporter construct. *Contrast Media Mol Imaging*. 2012;7:450-459.
29. Ziche M, Donnini S, Morbidelli L. Development of new drugs in angiogenesis. *Curr Drug Targets*. 2004;5:485-493.
30. Thomassin-Naggara I, Balvay D, Aubert E, et al. Quantitative dynamic contrast-enhanced MR imaging analysis of complex adnexal masses: a preliminary study. *Eur Radiol*. 2012;22:738-745.
31. Thomassin-Naggara I, Balvay D, Cuenod CA, Daraï E, Marsault C, Bazot M. Dynamic contrast-enhanced MR imaging to assess physiologic variations of myometrial perfusion. *Eur Radiol*. 2010;20:984-994.
32. Brito BOF, Ferreira E, Silva AE, Serakides R, Cassali GD. Aplicação do Software Corel DRAW® no estudo histomorfométrico de células neoplásicas [Corel DRAW Software application of the histomorphometric study of neoplastic cells.] Belo Horizonte: XIV Semana de Iniciação Científica da UFMG, 2005. https://www.ufmg.br/prpq/xivsic/trabalhos/Projetos_Atividade=3615.html. Accessed July 15, 2014.
33. Eichhorn ME, Kleespies A, Angele MK, Jauch KW, Bruns CJ. Angiogenesis in cancer: molecular mechanisms, clinical impact. *Langenbecks Arch Surg*. 2007;392:371-379.
34. Akbarzadeh A, Rezaei-Sadabady R, Davaran S, et al. Liposome: classification, preparation, and applications. *Nanoscale Res Lett*. 2013;8:102.
35. Deshpande PP, Biswas S, Torchilin VP. Current trends in the use of liposomes for tumor targeting. *Nanomedicine*. 2013;8:1509-1528.
36. Perche F, Torchilin VP. Recent trends in multifunctional liposomal nanocarriers for enhanced tumor targeting. *J Drug Deliv*. 2013;2013:705265.
37. Leite EA, Souza CM, Carvalho-Júnior AD, et al. Encapsulation of cisplatin in long-circulating and pH-sensitive liposomes improves its antitumor effect and reduces acute toxicity. *Int J Nanomedicine*. 2012;7:5259-5269.
38. De Barros AL, Mota LD, Soares DC, et al. Long-circulating, pH-sensitive liposomes versus long-circulating, non-pH-sensitive liposomes as a delivery system for tumor identification. *J Biomed Nanotechnol*. 2013;9:1636-1643.

39. Browder T, Butterfield CE, Kräling BM, et al. Antiangiogenic scheduling of chemotherapy improves efficacy against experimental drug-resistant cancer. *Cancer Res*. 2000;60: 1878-1886.
40. Drixler TA, Borel Rinkes IH, Ritchie ED, van Vroonhoven TJ, Gebbink MF, Voest EE. Continuous administration of angiostatin inhibits accelerated growth of colorectal liver metastases after partial hepatectomy. *Cancer Res*. 2000;60:1761-1765.
41. Kisker O, Becker CM, Prox D, et al. Continuous administration of endostatin by intraperitoneally implanted osmotic pump improves the efficacy and potency of therapy in a mouse xenograft tumor model. *Cancer Res*. 2001;61: 7669-7674.
42. Morishita T, Mii Y, Miyauchi Y, et al. Efficacy of the angiogenesis inhibitor O-(chloroacetyl-carbamoyl) fumagillol (AGM-1470) on osteosarcoma growth and lung metastases in rats. *Jpn J Clin Oncol*. 1995;25:25-31.
43. Jain RK. Normalization of tumor vasculature: an emerging concept in antiangiogenic therapy. *Science*. 2005;307: 58-62.
44. Goel S, Duda DG, Xu L, et al. Normalization of the vasculature for treatment of cancer and other diseases. *Physiol Rev*. 2011;91:1071-1121.
45. Jain RK. Delivery of molecular medicine to solid tumors: lessons from in vivo imaging of gene expression and function. *J Control Release*. 2001;74:7-25.
46. O'Connor JP, Carano RA, Clamp AR, et al. Quantifying antivascular effects of monoclonal antibodies to vascular endothelial growth factor: insights from imaging. *Clin Cancer Res*. 2009;15:6674-6682.
47. Kelland LR. Of mice and men: values and liabilities of the athymic nude mouse model in anticancer drug development. *Eur J Cancer*. 2004;40:827-836.
48. Corbett T, Polin L, Lorusso P, et al. In vivo methods for screening and preclinical testing. In: Teicher BA, Andrews PA, eds. *Anticancer Drug Development Guide: Preclinical Screening, Clinical Trials and Approval*. Totowa, NJ: Humana Press; 2004:99-123.
49. Gasparini G, Longo R, Fanelli M, Teicher BA. Combination of antiangiogenic therapy with other anticancer therapies: results, challenges, and open questions. *J Clin Oncol*. 2005;23:1295-1311.
50. Kerbel R, Folkman J. Clinical translation of angiogenesis inhibitors. *Nat Rev Cancer*. 2002;2:727-739.
51. Kudelka AP, Verschraegen CF, Loyer E. Complete remission of metastatic cervical cancer with the angiogenesis inhibitor TNP-470. *N Engl J Med*. 1998;338:991-992.